Constraining the calculation of ^{234,236,238}U(n,γ) cross sections with measurements of the γ-ray spectra at the DANCE facility

J. L. Ullmann, T. Kawano, B. Baramsai, T. A. Bredeweg, A. Couture, R. C. Haight, M. Jandel, J. M. O'Donnell, R. S. Rundberg, D. J. Vieira, J. B. Wilhelmy, M. Krtička, J. A. Becker, A. Chyzh, C. Y. Wu, and G. E. Mitchell

Constraining the calculation of ^{234,236,238}U(n,γ) cross sections with measurements of the gamma-ray spectra at DANCE

J.L. Ullmann, T. Kawano, B. Baramsai, T.A. Bredeweg, A. Couture, R.C. Haight,
M. Jandel,* J.M. O'Donnell, R.S. Rundberg, D.J. Vieira, and J.B. Wilhelmy
Los Alamos National Laboratory, Los Alamos, New Mexico 87545

M. Krtička
Charles University, Prague, Czech Republic 18000

J.A. Becker, A. Chyzh, C.Y. Wu
Lawrence Livermore National Laboratory, Livermore, California 94550

G.E. Mitchell
North Carolina State University, Raleigh, NC 27607
(Dated: August 14, 2017)

The cross section for neutron capture in the continuum region has been difficult to calculate accurately. Previous results for ^{238}U show that including an M1 scissors-mode contribution to the photon strength function resulted in very good agreement between calculation and measurement. This paper extends that analysis to ^{234,236}U by using gamma-ray spectra measured with the DANCE detector to constrain the photon strength function used to calculate the capture cross section. Calculations using a strong scissors-mode contribution reproduced the measured γ-ray spectra and were in excellent agreement with the reported cross sections for all three isotopes.

I. INTRODUCTION

An accurate knowledge of neutron capture cross sections on the actinides is important for many applied programs. In addition, an understanding of the physics needed to calculate these cross sections will enable extrapolation of the calculations to nuclides which are difficult to measure directly, such as ^{237,239}U. There are several measurements of the ^{234,236,238}U(n,γ) cross sections both in the keV region and the resolved resonance region, and several new and more accurate measurements of the cross section are in progress [1]. Calculations of the cross section in the unresolved resonance region from first principles have been notoriously difficult, however, and factors of two or more between the calculation and measurement are not uncommon.

The probability for γ decay in cross section calculations is described by the average gamma decay width $\langle \Gamma_\gamma \rangle$ which depends on the nuclear level density (NLD) and photon strength functions (PSF's) for all energies below the energy of the capturing state. Normalizing calculations to the measured $\langle \Gamma_\gamma \rangle$ and s-wave level spacing D_0 can result in reasonable values for the capture cross section when reliable values for those quantities are available.

It was previously shown for ^{238}U that including the M1 scissors mode resonance in addition to the E1 Giant Dipole Resonance in the photon strength functions not only resulted in an accurate calculation of the γ-ray

spectra, but also a very accurate calculation of the capture cross section in the fast-neutron energy range [2]. In this paper we extend the analysis to include ^{234,236}U. We measured gamma cascade spectra from a few well-resolved $J^\pi = 1/2^+$ resonances and compared them to calculations in order to constrain the photon strength functions, which were then used to calculate capture cross sections. The calculated cross sections are compared to evaluated cross sections [3] and representative data.

II. EXPERIMENT AND DATA PROCESSING

The measurements were done using the Detector for Advanced Neutron Capture Experiments (DANCE) at the Los Alamos Neutron Science Center. Briefly, DANCE is located on Flight Path 14 at the Lujan Neutron Scattering Center at 20.25 m from the upper-tier water moderator. DANCE is a nearly 4π γ-ray calorimeter composed of a spherical array of 160 BaF$_2$ crystals, each with a volume of 734 cm^3. The target position is surrounded by a ^{6}LiH sphere to attenuate scattered neutrons. The data acquisition system used two 8-bit, 2 ns/channel transient digitizers per crystal. Each digitizer had a range of 250 μsec. The time dispersion between crystal pairs was about 2 ns FWHM, and a window of ± 10 ns was used to identify events.

The neutron flux was monitored by three neutron detectors 2 m downstream of the target location. The flux at the monitor location was roughly 1 x 10^{-4} E$^{-1.033}$ neutrons/(cm^2 eV s) for a proton current of 100 μA, where E is the neutron energy in eV. The uranium targets were electroplated on a 2.5 μm Ti backing foil and

---

* Current Address: Univ. Massachusetts, Lowell, MA 01854

TABLE I. Target Parameters

Target	Thickness (mg/cm^2)	Q value (MeV)	Q-value Window (MeV)
^{234}U	1.00	5.30	4.80 - 5.80
^{236}U	1.29	5.13	4.63 - 5.63
^{238}U	2.27	4.81	4.16 - 5.46

enclosed in a target holder with 76 μm thick Kapton entrance and exit windows. The target thicknesses are shown in Table I.

Several γ rays can be emitted from a capture event, and a single γ ray interacting in DANCE can deposit energy in several adjacent crystals because of pair production and Compton scattering. Signals in adjacent crystals are summed together as a "cluster," and it has been shown that the energy (E_{cl}) and multiplicity (M_{cl}) of the cluster are proportional to the actual γ-ray energy and multiplicity [4]. The total deposited γ-ray energy summed over all crystals is shown in the summed-energy spectrum, which has a peak corresponding to the capture Q value and a low-energy tail due to incomplete detection of the γ-ray cascade. The multi-step cascade spectra (MSC), which consist of the individual E_{cl} energies for a given M_{cl}, were obtained by gating on a Q-value window on the summed-energy spectra. The MSC and summed-energy spectra are shown in Section III, and the Q-value windows are shown in Table I.

In this paper we study the multi-step cascade spectra for various multiplicities obtained by gating on isolated s-wave ($J^\pi = 1/2^+$) resonances below about 100 eV. For these neutron energies, the dominant background was due to gammas from the target backing and windows plus ambient gammas. The background was measured with targets consisting of the Ti backing foils only, and subtracted. More details are given in ref. [2].

III. COMPARISON OF EXPERIMENTAL AND SIMULATED SPECTRA

A. Calculations of Gamma-ray spectra

The measured summed-energy and MSC spectra are compared to calculated spectra using a forward-modeling approach. Model calculations of the spectra were made using the Monte-Carlo code DICEBOX [5] to generate γ cascades which were then processed through a well-tested GEANT4 model [6] of the DANCE array to account for the detector response. Simulated spectra were obtained using the same data-reduction cuts as applied to the measured data. This approach can serve as a verification of different models but it can not be easily used for predicting the best PSFs and LD models.

DICEBOX uses the measured levels from the Evaluated Nuclear Structure Data File (ENSDF) [7] up to critical energies of E_{crit} = 820, 760, and 830 keV for

^{235,237,239}U, respectively, and generates levels based on a nuclear level-density formula above E_{crit}. Individual transition probabilities between each pair of levels a and b are then simulated using partial radiation widths calculated as

$$\Gamma_{ab} = \sum_{XL} y_{XL}^2 [E_a - E_b]^{2L+1} \frac{f_{XL}(E_a - E_b)}{\rho(E_a, J_a^\pi)} \quad (1)$$

where ρ is the nuclear level density, f_{XL} is the photon strength function for transitions with multipolarity L and transition type X ($X \equiv E$ or M for electric or magnetic transitions), and y_{XL} is a random number taken from a normal distribution with zero mean and unit variance to account for Porter-Thomas fluctuations. In reality, only E1, M1, and E2 transitions are considered. Internal electron conversion is explicitly taken into account using the BRICC database [8]. Porter-Thomas fluctuations can lead to an extremely large number of different artificial nuclei which are called "nuclear realizations." Different nuclear realizations lead to different predicted summed-energy and MSC spectra – the difference is preserved in the GEANT4 simulations of the detector response. The range of predictions, corresponding to the average $\pm$ one sigma obtained from 20 nuclear realizations each consisting of 10^6 cascades, is shown in the figures below.

The shape of the γ-ray spectra simulated by DICEBOX is sensitive to the relative strength of the various E1 and M1 components of the photon strength function, but the absolute normalization of the spectra is not determined. Therefore the simulated spectra must be normalized to experiment, and a single normalization factor for each isotope allows comparison of the shapes of MSC spectra and multiplicity distribution. The normalization was done using areas of the relatively structureless $M_{cl} = 4$ MSC spectra.

It was shown previously [2] that the γ-ray spectra in ^{238}U(n,γ) cannot be reproduced by using a photon strength function that is based only on the tail of the E1 Giant Dipole Resonance (GDR). Analyses of data on actinides using several methods, including the Oslo method [9], analysis of multi-step cascade spectra [2] and nuclear resonance fluorescence experiments (for example [10]) strongly indicate the presence of a resonance structure in the PSF near 2 MeV. This resonance structure is usually identified with the M1 scissors-mode resonance since it is consistent with the energy systematics of the scissors mode [11].

In the present work, calculations of γ-ray spectra were made using several models for the E1 and M1 photon strength functions and the nuclear level density. The PSF parameters used in the calculations described below are listed in Table II. In the table, E, σ, and Γ are the energy, strength, and width of the giant resonances, and subscript G refers to the GDR, PR to the pygmy resonance, SM to the scissors mode, and SF to the M1 spin-flip mode. All calculations also included E2 strength

parameterized as the isoscaler Giant Quadrupole Resonance with parameters from ref. [12]. The E2 strength had a negligible effect on the gamma-ray spectra.

B. Models based on Oslo data

The Oslo group has used an approach combining reaction kinematics of charged-particle induced reactions with measured γ-ray spectra to simultaneously determine the PSF's and NLD in several actinide nuclei, including the compound nuclei ^{237,238,239}U [9, 13, 14]. A strong double-humped scissors mode was reported. It's parameters were deduced by subtracting a smooth background from the total measured photon strength functions. This background was described by the extrapolated tail of the GDR, described by the Generalized Lorentzian Model (GLO) [15] with parameters taken from fits to the photoneutron yield data of Caldwell $et~al.$ [9, 16] with fixed temperature T=0.2 MeV, plus a "pygmy" E1 resonance and the M1 spin-flip resonance, each described by a standard Lorentzian (SLO). Note that the GLO is identical to the Enhanced Generalized Lorentzian (EGLO) [17] with k=1 used in ref. [9]. The photoneutron yield includes neutrons due to (γ, xn) and $\bar{\nu}(\gamma, f)$ reactions. The parameters of the GDR, together with the pygmy resonance parameters used in ref. [9] are listed in Table II.

The M1 components in ref. [9] were described by three Lorentzian-shape terms, whose parameters are also given in Table II. The double-humped structure between 2 and 3 MeV was attributed to the scissors mode while the resonance near 7 MeV to the spin-flip mode. These parameters are different from those used in our previous calculations for ^{238}U [2], which were based on the ^{233}Th parameters from ref. [13]. The Oslo-method PSF's used in our calculations are shown in ref. [9].

The nuclear level density measured by the Oslo Method could be described by a constant-temperature model with T= 0.40, 0.39 MeV and spin cutoff σ_c= 8.02, 7.84 at the neutron separation energy for ^{237}U and ^{239}U respectively [14]. The parameters for ^{237}U were also used for our ^{235}U calculations. These level densities from the Oslo method are shown in fig. 1. Also shown are the predicted level densities using the constant-temperature (CT) parameterizations of von Egidy and Bucurescu [19, 20] and the parameterization used in the CoH$_3$ code [21].

The DICEBOX calculations of the γ-ray spectra using the Oslo model are compared to the spectra measured for various resonances in fig. 3. The experimental spectra are acceptably reproduced for ^{236}U(n,γ), but the bump near 2 MeV is wider and less pronounced than observed for the ^{234,238}U(n,γ) simulations. A representative comparison of the experimental summed-energy spectra and those simulated with the Oslo model is shown in fig. 5 for the ^{236}U(n,γ) reaction. The summed-energy spectra of 236, 238U(n,γ) are acceptably reproduced, although the predicted multiplicity distribution does not perfectly
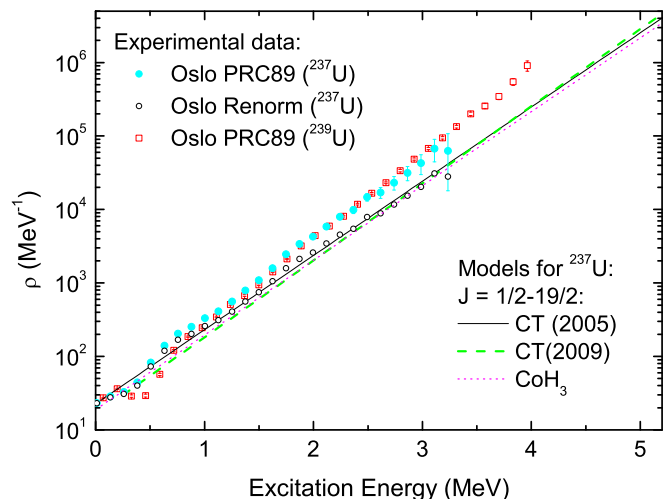
FIG. 1. (Color Online) Nuclear level density for ^{237,239}U obtained by the Oslo Method [14] compared to estimates from global fits for ^{237}U. "Oslo Renorm" designates the Oslo NLD renormalized as described in the text. The CT predictions are from refs. [19] and [20] and the CoH$_3$ prediction used an updated parameterization of the model in ref. [21].
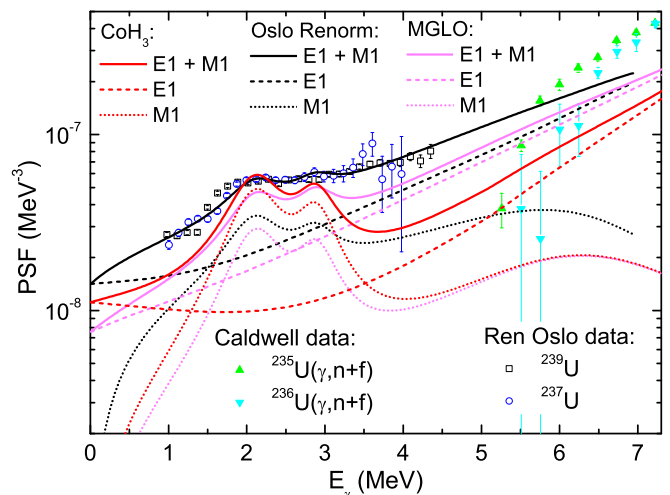
FIG. 2. (Color online) Comparison of PSF models used in simulations and the renormalized experimental data from Oslo [9]. "Renorm Oslo" designates the Oslo PSF renormalized as described in the text. See text for a description of the other models. The total photoneutron cross section data of Caldwell [16] are also shown

.

match the experiment. However, the reproduction of the summed-energy spectra for the ^{234}U(n,γ) reaction is less satisfactory.

The original Oslo normalization used the spin cutoff parameter $\sigma_c \approx 8$ at the neutron separation energy, which is consistent with the rigid-body value. Other phenomenological NLD models [19–21] predict a significantly smaller value, $\sigma_c \approx 5$. (Note that in ref. [19] the CT parameterization yields σ_c=4.80 while the back-shifted
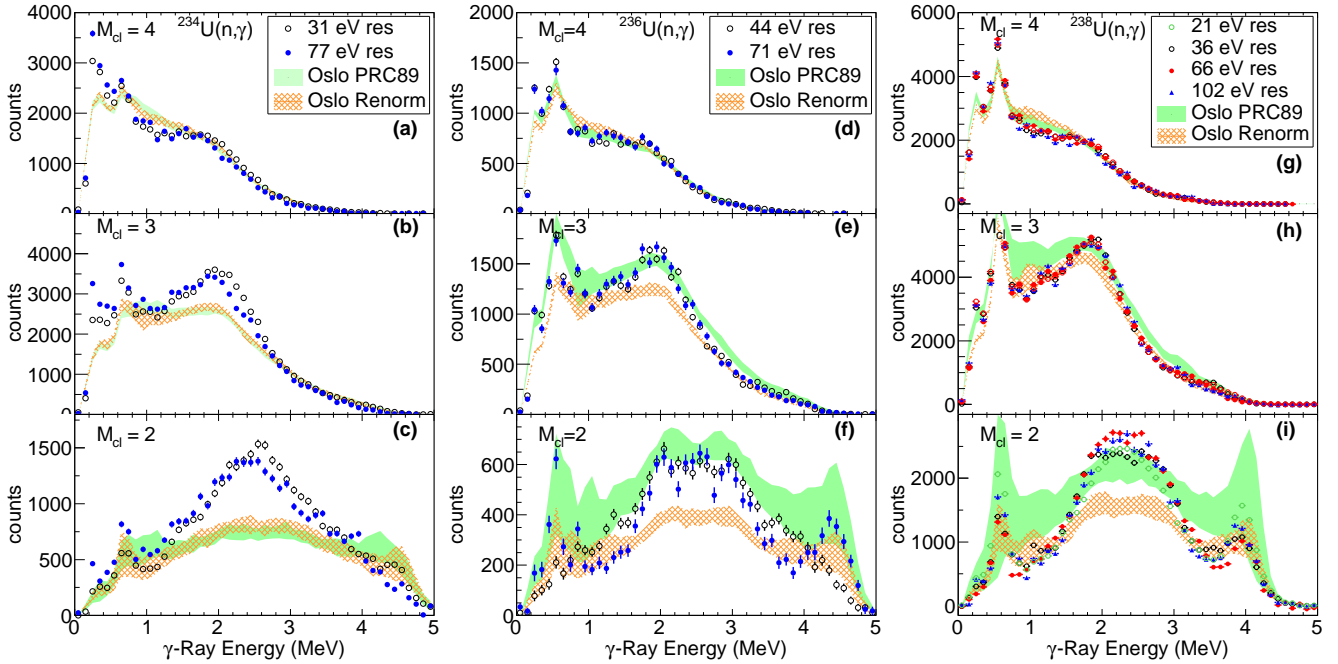
FIG. 3. (Color online) Measured γ-ray spectra for several $1/2^+$ resonances in ^{234,236,238}U(n,γ) compared to calculations made with photon strength-function and nuclear level-density parameters obtained from the Oslo method and by renormalizing the Oslo results as described in the text. The resonance energies are indicated in each panel. The y-axis counts are arbitrarily normalized.
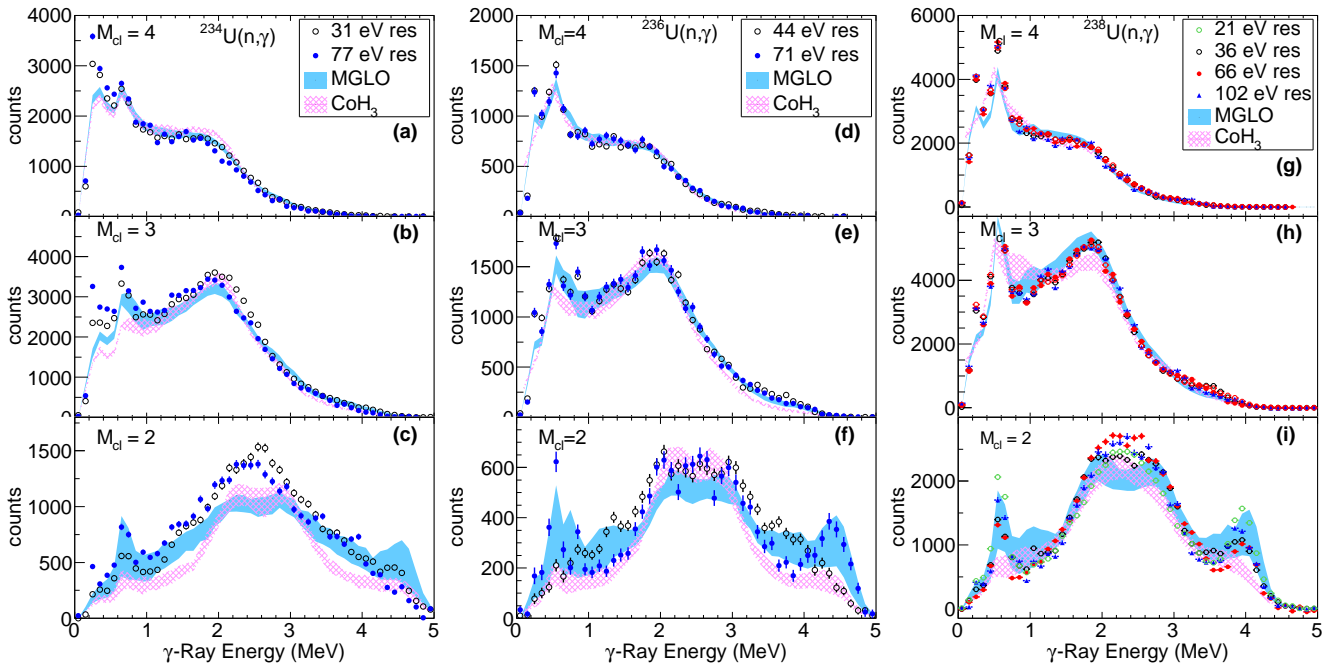
FIG. 4. (Color online) Measured γ-ray spectra for several $1/2^+$ resonances in ^{234,236,238}U(n,γ) compared to calculations made with photon strength-function and nuclear level-density parameters obtained from systematics used in the CoH$_3$ code and using the MGLO and CoH$_3$ models for the E1 strength. The resonance energies are indicated in each panel. The y-axis counts are arbitrarily normalized.
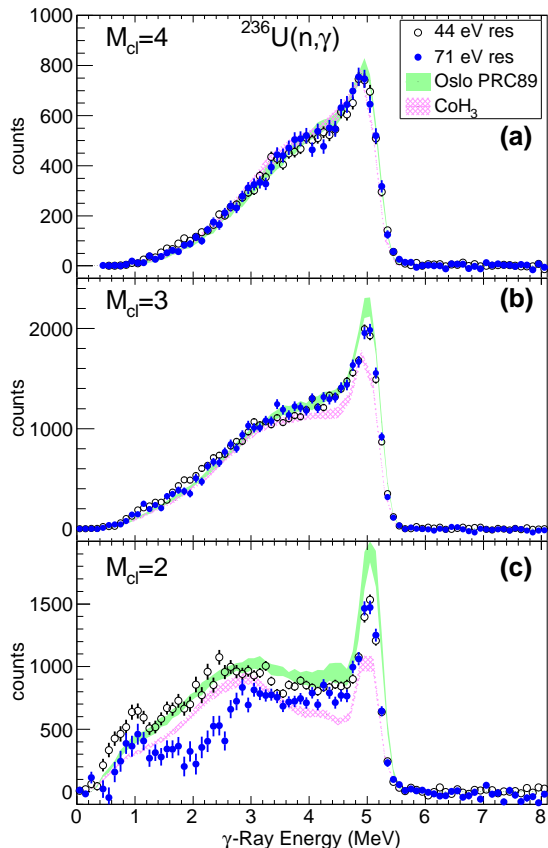
parameters.

FIG. 5. (Color online) Summed-energy spectra for two resonances in ^{236}U(n,γ) compared to calculations using the PSF and NLD from the Oslo method [9] and using the parameters in the CoH$_3$ code. The y-axis counts are arbitrarily normalized.

Fermi gas parameterization gives σ_c=7.84.) This change in σ_c would significantly change the normalization of the NLD and PSF's deduced in the Oslo method by changing the predicted fraction of $1/2^+$ neutron resonances.

We investigated the effect of renormalizing the original Oslo parameters to $\sigma_c \approx 5$. This change in the normalization of the level densities can be accounted for in the Oslo method by multiplying the total level density by a factor of $\exp(-0.25E_x)$, where E_x is the excitation energy. Such a change in the level density normalization also requires a renormalization of the PSF by $\exp(-0.25E_\gamma)$ to reproduce the Oslo experimental spectra [22] . The renormalized level density is shown in fig. 1. The renormalized PSF's from the Oslo method, with the absolute normalization adjusted to reproduce the experimental $\langle\Gamma_\gamma\rangle$ for ^{237}U and ^{239}U are shown in fig. 2. Simulations of the MSC spectra with the renormalized Oslo-based level densities and PSF's are also shown in Fig 3. For ^{236}U(n,γ) and ^{238}U(n,γ), the reproduction of the experimental spectra with the renormalized Oslo model is significantly worse than with the original Oslo

C. Models based on CoH$_3$ systematics

We next made simulations of the spectra based on systematics of the level density and photon strength function as used in calculations of the capture cross section with the CoH$_3$ code. For the E1 GDR component we used the GLO model with the E_γ-dependent prescription for the temperature (T) as proposed by Kopecky [15]: $T = \sqrt{(S_n - E_\gamma)/a}$, where S_n is the neutron separation energy and a is the level-density parameter. The GDR parameters were based on fits to the photoabsorption cross section, and were taken from the compilation of ref. [23]. The M1 PSF was represented by a sum of spin-flip and scissors-mode resonances each described by a standard Lorentzian shape. For the M1 scissors mode we used the resonance energies and widths from the Oslo parameterization for ^{237}U, but adjusted the resonance strengths to get the best agreement between experimental and simulated spectra, keeping the ratio of the two components the same as the Oslo result. The parameters are shown in Table II, and the PSF plotted in fig. 2. Note that the same scissors-mode parameters were used for all three nuclei. The resulting M1 strength was very strong. An acceptable description of the MSC spectra was obtained for values of $\Sigma B(M1)\uparrow$ ranging from 14 to 24 μ_N^2. The parameters listed in Table II and used in the simulations shown in figs. 4 and 5 correspond to $\Sigma B(M1)\uparrow = 18.8$ μ_N^2. This strength is significantly higher than $\Sigma B(M1)\uparrow = 9.1$ μ_N^2 in the original Oslo result. The level densities were based on the composite level-density formula of Gilbert and Cameron [25] with an updated parametrization [21]. The description of the multi-step cascade spectra are, in general, better than for the Oslo-based models especially for ^{234}U(n,γ). This is a consequence of the very strong scissors mode. For the ^{236}U(n,γ) summed-energy spectra shown in fig. 5, the CoH$_3$ and Oslo parameters provide an equivalently good description of the data.

D. Optimal description of γ spectra

The description of the γ-ray spectra using the models in Sections III B and III C is not perfect, and it is possible that a better description could be obtained by judicious selection of models for the E1 GDR low-energy tail and further adjustment of the M1 strength. The parameter space is very large and we have not made a systematic parameter search. In our limited search, we started by using for the E1 component the Modified Generalized Lorentzian form (MGLO) [26] with $k = 3$ and fixed temperature $T = 0.5$ MeV. This model provided a good description of the MSC spectra in well-deformed Gd nuclei [26–28]. The GDR parameters were taken from fits to ^{239}Pu photoabsorption cross section data in ref. [29].

The energies, widths, and ratio of the strengths of the two scissors-mode components were taken from the Oslo results for ^{237}U, while the overall strength was adjusted for the best reproduction of the experimental spectra. The same parameters were used for all three isotopes. The parameters for the GDR, spin-flip and scissors-mode resonances are given in Table II and the PSF's corresponding to this model are plotted in Fig. 2. A constant-temperature nuclear level density [19] was used. MSC spectra calculated with this model are shown in Figure 4. For these nuclei, the simulations based on the MGLO model and the GLO model using the CoH$_3$ parameters produced comparable results.

E.   Discussion

Comparison of the experimental and simulated spectra indicates that calculations based on the CoH$_3$ and MGLO models provide a significantly better description of the MSC spectra than the models based on the Oslo analysis, expecially for the M$_{cl}$=2 spectra. Both of these models infer $B(M1)$ for the scissors mode contribution to be significantly higher than proposed by the Oslo analysis and by nuclear resonance fluorescence in the adjacent ^{238}U nucleus [10]. However, it should be noted that it is very difficult to estimate the total strength from fluorescence experiments in nuclei with high level density.

Two observations can be made from the attempts to fit the spectra. First, attempts (not shown) to fit the spectra with a single Lorentzian scissors-mode resonance structure were not very successful, and the two-Lorentzian structure determined in the Oslo results seems to be required. Second, contrary to the situation in the rare-earth region [26–28], our calculations cannot conclusively determine the character of the resonance structure between 2 and 3 MeV. This is a consequence of the high NLD for levels with both parities. Nonetheless, the structure is consistent with other observations of the scissors mode.

IV.   CROSS SECTION CALCULATIONS

A.   Hauser-Feshbach Calculations

Cross section calculations were made using the statistical Hauser-Feshbach code CoH$_3$ [32]. The Hauser-Feshbach formula for neutron radiative capture has the schematic form

$$\sigma_{capt}(E_n) = \frac{\pi}{k_n^2} \sum_{J\Pi} g_c \frac{T_n T_\gamma}{T_n + T_\gamma} W_{n\gamma}, \quad (2)$$

where E_n is the energy of the incoming neutron, k_n is the neutron wave number, g_c is the statistical spin factor, T_n is the neutron transmission coefficient, T_γ is the lumped γ-ray transmission coefficient, $W_{n\gamma}$ is the width fluctuation correction factor, and the sum is over all allowed capture state spin and parity (J^Π) combinations. These indicies have been omitted from eq. (2) for clarity. Although the fission cross section is negligible in our energy range and omitted in eq. (2), the fission channel was included in the CoH$_3$ implementation. For calculating $W_{n\gamma}$ we use the model of Moldauer [33] with the Gaussian Orthogonal Ensemble parameterization [35]. The Englebrecht-Weidenmüller transformation [36] is performed to correctly account for the direct inelastic scattering channels in the width fluctuation calculation. We employed the coupled-channels optical potential of Soukhovitskii et al. [37] which is appropriate for the actinide region.

The lumped γ-ray transmission coefficient T_γ is calculated as

$$T_\gamma = \sum_{j^\pi X L} \int_0^{E'} 2\pi E_\gamma^{(2L+1)} f_{XL}(E_\gamma) \rho(E_x, j^\pi)\, dE_x \quad (3)$$

where $E' = S_n + E_n$, E_x is the excitation energy in the residual nucleus, S_n is the neutron separation energy, and $E_\gamma = S_n + E_n - E_x$ is the emitted γ-ray energy. The summation is over all allowed final-state spin and parity (j^π) combinations. The integral in Eq. (3) is replaced by a sum for discrete final states below E_{crit}. T_γ can be related to the experimental average s-wave radiation width $\langle \Gamma_\gamma \rangle$ and the average s-wave resonance spacing as D_0,

$$T_\gamma = 2\pi \frac{\langle \Gamma_\gamma \rangle}{D_0}. \quad (4)$$

The cross section depends on the absolute value of the strength function and the details of the level density and has often been difficult to calculate accurately. Relation (4) has often been used to normalize capture calculations when D_0 and $\langle \Gamma_\gamma \rangle$ have been experimentally determined.

In this work, no renormalization of T_γ to $\langle \Gamma_\gamma \rangle$ has been done. Cross sections were calculated using the PSF and NLD models described in Section III C. The results of the calculations are compared to representative data and the ENDF/B VII.1 evaluation [3] in Fig 6. For ^{238}U the calculation without the scissors mode contribution is also shown. Results for ^{238}U were published previously [2]; the present calculations use slightly different parameters for the M1 scissors mode than used in that work, but the difference is small. For ^{236}U, representative data from the EXFOR library [41] are shown, while for ^{234}U, no data were available in the EXFOR library. The measured cross sections and evaluations are very well represented by the calculations.

B.   Sensitivity to NLD and PSF

Although the role of different formulations for the nuclear level density and E1 strength function in calculating

TABLE II. Photon Strength Function parameters used in calculations. The parameters are described in the text. Note that there was a typographical error in ref. [9] for the cross section of the first scissors mode term in ^{239}U; the value should be 0.40 instead of 0.30 [42].

$E1$	E_{G_1} (MeV)	σ_{G_1} (mb)	Γ_{G_1} (MeV)	E_{G_2} (MeV)	σ_{G_2} (mb)	Γ_{G_2} (MeV)	E_{PR} (MeV)	σ_{PR} (mb)	Γ_{PR} (MeV)	
Oslo	11.40	572	4.20	14.40	1040	4.20	7.30	15.0	2.0	^{235,7,9}U [9]
CoH$_3$	11.50	315	2.60	14.09	431	4.51				^{235}U
CoH$_3$	11.48	318	2.59	14.06	435	4.50				^{237}U
CoH$_3$	11.47	319	2.59	14.03	439	4.50				^{239}U
MGLO	11.28	325	2.48	13.73	384	4.25				^{235,7,9}U [29]
$M1$	E_{SM_1} (MeV)	σ_{SM_1} (mb)	Γ_{SM_1} (MeV)	E_{SM_2} (MeV)	σ_{SM_2} (mb)	Γ_{SM_2} (MeV)	E_{SF} (MeV)	σ_{SF} (mb)	Γ_{SF} (MeV)	
Oslo	2.15	0.45	0.80	2.90	0.40	0.60	6.61	7.00	4.0	^{235,7}U [9]
Oslo	2.00	0.40	0.80	2.80	0.30	1.20	6.61	7.00	4.0	^{239}U [9]
CoH$_3$	2.15	1.05	0.80	2.90	0.93	0.60	6.61	1.50	4.0	^{235,7,9}U
MGLO	2.15	0.60	0.80	2.90	0.53	0.60	6.61	1.50	4.0	^{235,7,9}U
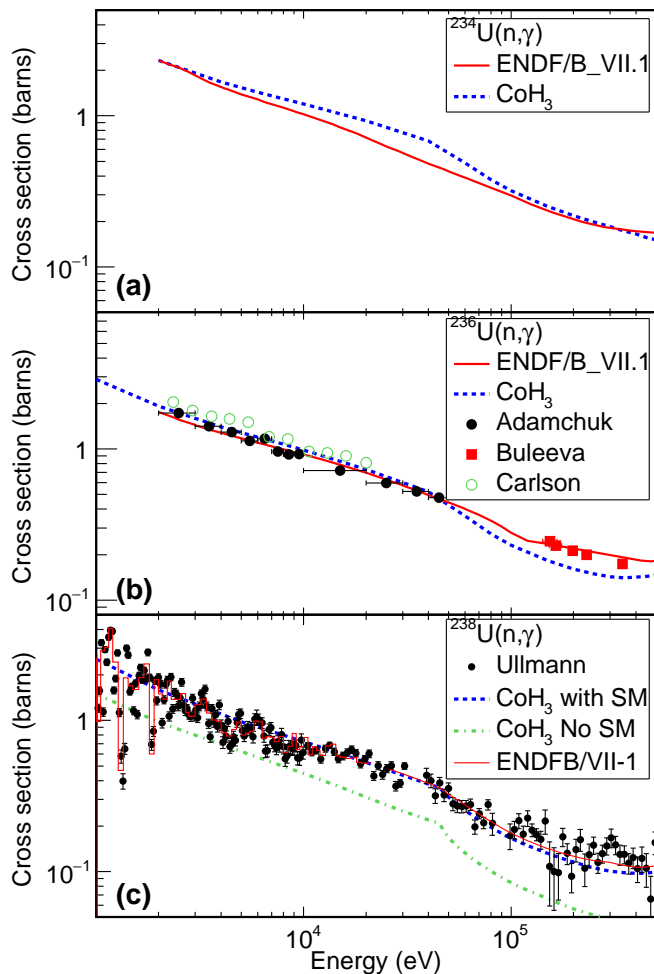
FIG. 6. (Color online) Calculated cross sections for ^{234,236,238}U(n,γ) compared to the ENDFB/VII-1 evaluation [3] and representative data. For ^{236}U, measurements by Adamchuk [40], Buleeva [39], and Carlson [38] are shown. The tabulated data were obtained from the EXFOR data base [41]. The ^{238}U(n,γ) results were published previously [2].

Γ_γ is complicated, we made a simple investigation of their effects. To do this, we calculated the $\langle\Gamma_\gamma\rangle$ corresponding to the decay of $1/2^+$ resonances just above the neutron separation energy using the DICEBOX algorithm. These calculations were done with different models and parameterizations, and can be compared to the experimental values.

The results are shown in Table III. The uncertainty indicated in parenthesis represents the expected fluctuation of Γ_γ from different nuclear realizations calculated by DICEBOX. The first three entries illustrate the effect of the level density. Three level-density formulations were tested while keeping the CoH$_3$ parameters for the PSF's fixed at the values in Table II. The calculated $\langle\Gamma_\gamma\rangle$ varied by as much as a factor of 1.7 for ^{239}U, about 1.3 for ^{237}U, and 1.2 for ^{235}U. Capture cross sections using these models would show a comparable variation. The influence of the NLD on the calculated $\langle\Gamma_\gamma\rangle$ is very similar using other models of the PSF. The sensitivity of $\langle\Gamma_\gamma\rangle$ to the NLD indicates that care must be taken in choosing the NLD formulation used in cross-section calculations.

The next three entries show the results using other tested models. The values of Γ_γ were calculated using the published Oslo parameters, the "renormalized" Oslo parameters, and the MGLO form for the E1 PSF. The absolute normalization for all PSF's corresponds to fig. 2.

The effect of using different parameter sets for E1 GDR was also investigated. To do this, the NLD, M1 and E2 PSF parameters were kept fixed at those from the CoH$_3$ parameterization. Simulations were made for ^{237,239}U compound nuclei using the GLO model for the E1 PSF with parameters for ^{236,238}U from Veyssiere [43], Gurevich [44], and Dietrich [29], as well as the CoH$_3$ values shown in Table II. The calculated $\langle\Gamma_\gamma\rangle$ values ranged from 22 to 26 meV. The contribution of the M1 scissors mode was about 13 meV and the contribution from the M1 spin-flip plus E2 modes was about 3 meV for both nuclei. The E1 contribution ranged from 6 to 10 meV; the calculation made using the CoH$_3$ parameters listed

TABLE III. Total radiation widths Γ_γ of s-wave resonances ($J^\Pi = 1/2^+$) obtained with different models of PSFs and NLD parametrizations (See text). The model combinations labeled with the asterisk were used in the simulations shown in figs. 3 - 5

Model		Γ_γ (meV)		
PSF	NLD	^{235}U	^{237}U	^{239}U
CoH$_3$	[19]	23.7(5)	19.0(5)	16.6(5)
CoH$_3$	[20]	27.4(18)	17.5(4)	13.4(6)
CoH$_3^*$	[21]	26.5(6)	23.3(7)	23.3(6)
Oslo*		20.0(3)	21.2(8)	18.9(5)
Oslo Renorm*		29.5(7)	24.1(9)	22.0(7)
MGLO*	[19]	21.5(6)	17.5(6)	16.2(5)
Evaluation	[45]	25.3(10)	23.4(8)	23.36(31)

in Table II gave 7.5 meV for ^{237}U and 6.7 meV for ^{239}U.

Varying the GDR parameter sets produced nearly a 50% difference in the value of the E1 contribution to $\langle\Gamma_\gamma\rangle$. However, the total E1 contribution was only about 30% for the model in Sec. III C and 55% for the model in Sec. III D. Therefore, use of the different GDR parameters did not strongly influence $\langle\Gamma_\gamma\rangle$ for the even U isotopes considered here.

V. CONCLUSIONS

The cross section for neutron radiative capture has been difficult to calculate accurately from first principles. One of the main sources of uncertainty is in the calculation of the γ-ray transmission coefficient or total radiation width of the capturing state, which is calculated as the overlap of the nuclear level density and the photon strength function. It is usually assumed that E1 transitions play a dominant role in the radiative decay, with additional contributions from the M1 spin-flip and E2 isoscaler quadrupole giant resonances. However, our analysis of γ-ray spectra from radiative neutron capture through s-wave resonances in ^{234,236,238}U indicates that a significant contribution to the Γ_γ comes from a resonance structure at E_γ from 2 to 3 MeV, which is identified with the M1 scissors-mode expected in deformed nuclei. This contribution is even higher than that determined by the Oslo Method for U nuclei. When this additional strength is added to standard models for the E1 PSF and NLD in the CoH$_3$ code, the calculated radiative capture cross sections, with no additional renormalization, are in very good agreement with the measured or evaluated values for ^{234,236,238}U(n,γ).

[1] B. Baramsai, et al., accepted for publication Phys. Rev. C.

[2] J. L. Ullmann, T. Kawano, T. A. Bredeweg, A. Couture, R. C. Haight, M. Jandel, J. M. O'Donnell, R. S. Rundberg, D. J. Vieira, J. B. Wilhelmy, J. A. Becker, A. Chyzh, C. Y. Wu, B. Baramsai, G. E. Mitchell, and M. Krtička, Phys. Rev. C **89**, 034603 (2014).

[3] M. B. Chadwick, M. Herman, P. Obložinský, M.E. Dunn, Y. Danon, A.C. Kahler, D.L. Smith, B. Pritychenko, G. Arbanas, R. Arcilla, R. Brewer, D.A. Brown, R. Capote, A.D. Carlson, Y.S. Cho, H. Derrien, K. Guber, G.M. Hale, S. Hoblit, S. Holloway, T.D. Johnson, T. Kawano, B.C. Kiedrowski, H. Kim, S. Kunieda, N.M. Larson, L. Leal, J.P. Lestone, R.C. Little, E.A. McCutchan, R.E. MacFarlane, M. MacInnes, C.M. Mattoon, R.D. McKnight, S.F. Mughabghab, G.P.A. Nobre, G. Palmiotti, A. Palumbo, M.T. Pigni, V.G. Pronyaev, R.O. Sayer, A.A. Sonzogni, N.C. Summers, P. Talou, I.J. Thompson, A. Trkov, R.L. Vogt, S.C. van der Marck, A. Wallner, M.C. White, D. Wiarda, and P.G. Young, Nuclear Data Sheets **112**, 2887 (2011).

[4] M. Jandel et al., Nucl. Instrum. Methods B **261**, 1117 (2007).

[5] F. Bečvář, Nucl. Instr. Meth. A **417**, 434 (1998).

[6] M. Jandel, T.A. Bredeweg, A. Couture, M.M. Fowler, E.M. Bond, M.B. Chadwick, R.R. Clement, E.-I. Esch, J.M. O'Donnell, R. Reifarth, R.S. Rundberg, G.S. Rusev, P. Talou, I. Stetcu, J.L. Ullmann, D.J. Vieira, J.B. Wilhelmy, J.M. Wouters, R.A. Macri, C.Y. Wu, and J.A. Becker, Nucl. Instru. and Meth. B **261**, 117 (2007).

[7] www.nndc.bnl.gov/ensdf.

[8] T. Kibedi, T.W. Burrows, M.B. Trzhaskovskaya, P.M. Davidson, and C.W. Nestor, Jr., Nucl. Instru. and Meth. A **589**, 202 (2008). Available at bricc.anu.edu.au.

[9] M. Guttormsen, L.A. Bernstein, A. Görgen, B. Jurado, S. Siem, M. Aiche, Q. Ducasse, F. Giacoppo, F. Gunsing, T.W. Hagen, A.C. Larsen, M. Lebois, B. Leniau, T. Renstrøm, S.J. Rose, T.G. Tornyi, G.M. Tveten, M. Weideking, and J.N. Wilson, Phys. Rev. C **89**, 014302 (2014).

[10] S.L. Hammond, A.S. Adekola, C.T. Angell, H.J. Karwowski, E. Kwan, G. Rusev, A.P.Tonchev, W. Tornow, C.R. Howell, and J.H. Kelley, Phys. Rev. C **85**, 044302 (2012).

[11] K. Heyde, P. von Neuman-Cosel, and A. Richter, Rev. Mod. Phys. **82**, 2366 (2010).

[12] W.V. Prestwich, M.A. Islam, and T.J. Kennett, Z. Phys. **A315**, 103 (1984).

[13] M. Guttormsen, L.A. Bernstein, A. Bürger, A. Görgen, F. Gunsing, T.W. Hagen, A.C. Larsen, T. Renstrøm, S. Siem, M. Weideking, and J.N. Wilson, Phys. Rev. Lett. **109**, 162503 (2012).

[14] M. Guttormsen, B. Jurado, J.N. Wilson, M. Aiche, L.A. Bernstein, Q. Ducasse, F. Giacoppo, A. Görgen, F. Gunsing, T.W. Hagen, A.C. Larsen, M. Lebois, B. Leniau, T. Renstrøm, S.J. Rose, S. Siem, T. Tornyi, G.M. Tveten, and M. Wiedeking, Phys. Rev. C **88**, 024307 (2013).

[15] J. Kopecky and M. Uhl, Phys. Rev. C **41**, 1941 (1990).

[16] J. T. Caldwell, E. J. Dowdy, B. L. Berman, R. A. Alvarez, and P. Meyer, Phys. Rev. C **21**, 1215 (1980).

[17] J. Kopecky, M. Uhl, R. E. Chrien, Phys. Rev. C, **47**, 312 (1993).

[18] J. Kopecky and R.E. Chrien, *Nucl. Phys.* **A468** (1987) 285.

[19] T. von Egidy and D. Bucurescu, Phys. Rev. C **72**, 044311 (2005).

[20] T. von Egidy and D. Bucurescu, Phys. Rev. C **80**, 054310 (2009).

[21] T. Kawano, S. Chiba, and H. Koura, J. Nucl. Sci. Technol. **43**,1 (2006).

[22] A.C. Larsen, M. Guttormsen, M. Krticka, E. Betak, A. Burger, A. Gorgen, H.T. Nyhus, J. Rekstad, A. Schiller, S. Siem, H.K. Toft, G.M. Tveten, A.V. Voinov, and K. Wikan, Phys. Rev. C **83**, 034315 (2011).

[23] M. Herman, R. Capote, M. Sin, A. Trkov, B.V. Carlson, P. Oblozinsky, C.M. Matoon, H. Wienke, S. Hoblit, Y.-S. Cho, G. Nobre, and V. Zerkin, *EMPIRE-3.2 Malta, Modular system for nuclear reaction calculations and nuclear data evaluation Users Manual,* Tech. Report INDC(NDS)-0603 (International Atomic Energy Agency, 2013).

[24] R. Capote, M. Herman, P. Obložinský, P. G. Young, S. Goriely, T. Belgya, A. V. Ignatyuk, A. J. Koning, S. Hilaire, V. A. Plujko, M. Avrigeanu, O. Bersillon, M. B. Chadwick, T. Fukahori, Z. Ge, Y. Han, S. Kailas, J. Kopecky, V. M. Maslov, G. Reffo, M. Sin, E. Sh. Soukhovitskii, P. Talou, "RIPL — Reference Input Parameter Library for Calculation of Nuclear Reactions and Nuclear Data Evaluations," *Nucl. Data Sheets,* **110**, 3107 (2009); *Handbook for calculations of nuclear reaction data, RIPL-2, Reference Input Parameter Library,* IAEA-TECDOC-1506, International Atomic Energy Agency (2006).

[25] A. Gilbert and A.G.W. Cameron, Can. J. Phys **43**, 1446 (1965).

[26] J. Kroll, B. Baramsai, G.E. Mitchell, U. Agvaanluvsan, F. Bečvář, T.A. Bredeweg, A. Chyzh, A. Couture, D. Dashdorj, R.C. Haight, M. Jandel, A.L. Keksis, M. Krtička, J.M. O'Donnell, W. Parker, R.S. Rundberg, J.L. Ullmann, S. Valenta, D.J. Vieira, C. Walker, and C.Y. Wu. Phys. Rev. C **88**, 034317 (2013).

[27] B. Baramsai, J. Kroll, G.E. Mitchell, U. Agvaanluvsan, F. Bečvář, T.A. Bredeweg, A. Chyzh, A. Couture, D. Dashdorj, R.C. Haight, M. Jandel, A.L. Keksis, M. Krtička, J.M. O'Donnell, R.S. Rundberg, J.L. Ullmann, D.J. Vieira, and C.L. Walker. Phys Rev. C **87**, 044609 (2013).

[28] A. Chyzh, B. Baramsai, J.A. Becker, F. Bečvář, T.A. Bredeweg, A. Couture, D. Dashdorj, R.C. Haight, M. Jandel, J. Kroll, M. Krtička, G.E. Mitchell, J.M. O'Donnell, W. Parker, R.S. Rundberg, J.L. Ullmann, D.J. Vieira, C.L. Walker, J.B. Wilhelmy, J.M. Wouters, and C.Y. Wu. Phys. Rev. C **84**, 014306 (2011).

[29] S.S. Dietrich and B.L. Berman, Atomic Data and Nuclear Data Tables **28**, 199 (1988).

[30] B.L. Berman, J.T. Caldwell, E.J. Dowdy, S.S. Dietrich, P. Meyer, R.A. Alvarez, Phys. Rev. C **34**, 2201 (1986).

[31] K. Heyde, P. von Neumann-Cosel, and A. Richter, Rev. Mod. Phys. **82**, 2365 (2010).

[32] T. Kawano, P. Talou, M. B. Chadwick, T. Watanabe, J. Nucl. Sci. Technol. **47**, 462 (2010)

[33] P.A. Moldauer, Nucl. Phys. A **344**, 185 (1980).

[34] T. Kawano, P. Talou, Nuclear Data Sheets **118**, 183 (2014).

[35] T. Kawano, P. Talou, H.A. Weidenmuller, Phys. Rev. C **92**, 044617 (2015).

[36] T. Kawano, R. Capote, S. Hilaire, and P. Chau Huu-Tai, Phys. Rev. C **94**, 014612 (2016).

[37] E.S. Soukhovitskii, R. Capote, J. M. Quesada, S. Chiba, Phys. Rev. C **72**, 024604 (2005).

[38] A.D. Carlson, S.J. Friesenhahn, W.M. Lopez, and M.P. Fricke, Nucl. Phys. A **141**, 577 (1970).

[39] N.N. Buleeva, A.N. Davletshin, A.O. Tipunkov, S.V. Tikhonov, and V.A. Tolstikov, Sov. At. Energy **65**, 920 (1988).

[40] Y.V. Adamchuk, M.A. Voskanyan, G.V. Muradyan, and V.A. Stepanov, Sov. At. Energy **65**, 930 (1988).

[41] The EXFOR data base is available at www.nndc.bnl.gov/exfor. See also N. Otuka,*et al.*, Nuclear Data Sheets **120**, 272 (2014).

[42] M. Guttormsen, private communication.

[43] A. Veyssiere, H. Beil, R. Bergere, P. Carlos, A. Leprete, A. de Miniac, Nucl. Phys. **A227**, 513 (1974).

[44] G.M. Gurevich, L.E. Lazareva, V.M. Mazur, G.V. Solodukhov, and B.A. Tulupov, Nucl. Phys. **A273**, 326 (1976).

[45] S. F. Mughabghab, "Atlas of Neutron Resonances, Resonance Parameters and Thermal Cross Sections, Z=1–100," Elsevier (2006).